JACC: CASE REPORTS VOL. 3, NO. 13, 2021

CASE REPORT

ADVANCED

CLINICAL CASE SERIES: TECHNICAL CORNER

Multimodality Imaging for Evaluation of Bicaval Valved Stent Implantation in Severe Tricuspid Regurgitation

Mirjam G. Wild, MD,[a] Martin Gloeckler, MD,[b] Kerstin B. Wustmann, MD,[a] Sophie A. Erne, MD,[a] Hanna Grogg, MD,[a] Adrian T. Huber, MD,[c] Stephan Windecker, MD,[a] Fabien Praz, MD,[a] Christoph Gräni, MD, PhD[a]

ABSTRACT

Preprocedural planning and postprocedural evaluation after transcatheter treatment of severe tricuspid regurgitation remain challenging and require further research and standardization. We illustrate the use of multimodality imaging techniques in 3 patients undergoing implantation of a novel custom-made bicaval valved stent for symptomatic treatment of severe tricuspid regurgitation. (**Level of Difficulty: Advanced.**) (J Am Coll Cardiol Case Rep 2021;3:1512–1518)

INTRODUCTION

The implantation of a bicaval valved stent has recently been proposed as a therapeutic option in patients with severe tricuspid regurgitation (TR) who are at high surgical risk and ineligible for other transcatheter treatment systems (1,2). This custom-made prosthesis aims to relieve symptoms of right-sided heart failure by preventing backflow into the systemic venous system. Imaging of the tricuspid valve and right ventricle (RV) is particularly challenging given the anatomical complexity, technical limitations, and lack of standardization. We illustrate the use of multimodality imaging techniques in 3 symptomatic patients with severe secondary TR who underwent implantation of a novel custom-made bicaval valved stent (Medira AG). Because of the large coaptation gap and annular dimensions, as well as the high surgical risk, all patients were deemed ineligible for other treatment options (ie, surgical repair, transcatheter leaflet approximation, or direct annuloplasty). Retrospective collection of study data and was waived by our local ethics committee (KEK Bern 2021-01140, Inselspital, University of Bern, Switzerland).

LEARNING OBJECTIVES

- To define the crucial role of standardized preprocedural and postprocedural multimodality imaging and its synergistic value for novel tricuspid valve devices.
- To demonstrate the advantages of 4D CT for the assessment of device success and detection of potential device malfunction.
- To appreciate the necessity of collaboration among interventional cardiologists, imaging specialists, and engineers to develop and evaluate novel and innovative valve therapies.

From the [a]Department of Cardiology, Inselspital, Bern University Hospital, University of Bern, Bern, Switzerland; [b]Department of Cardiology, Center for Congenital Heart Disease, Inselspital, Bern University Hospital, University of Bern, Bern, Switzerland; and the [c]Department of Diagnostic, Interventional, and Pediatric Radiology, Inselspital, Bern University Hospital, University of Bern, Bern, Switzerland.

The authors attest they are in compliance with human studies committees and animal welfare regulations of the authors' institutions and Food and Drug Administration guidelines, including patient consent where appropriate. For more information, visit the Author Center.

Manuscript received April 26, 2021; revised manuscript received June 22, 2021, accepted July 12, 2021.

ISSN 2666-0849 https://doi.org/10.1016/j.jaccas.2021.07.009

CASE 1

An 82-year-old female patient was referred for evaluation of treatment options for symptomatic massive TR (Video 1A). She was symptomatic with dyspnea at rest (New York Heart Association [NYHA] functional class IV), she required home oxygen, and she had pronounced anasarca, pleural effusions, ascites, and loss of appetite, despite maximal diuretic therapy. Multimodality imaging was used to assess her eligibility for bicaval stent implantation (**Tables 1 and 2, Figure 1**). Stent implantation was uneventful (**Figures 2A to 2C,** Videos 2A and 2B), with improvement of symptoms and resolution of oxygen dependency, body weight loss, and complete relief of peripheral edema and ascites (**Table 2**). On echocardiography, we observed correct device position with systolic compression of the stent in the right atrium (RA) without an impact on valve competency or the appearance of paravalvular leakage (Video 1B). Follow-up imaging included 4-dimensional (4D) computed tomography (CT) and cardiac magnetic resonance (CMR) to assess device position, RV volumes, and myocardial function, including strain imaging (MEDIS Suite v.3.0, Circle, cvi42). At follow-up, CMR and CT showed a reduction of RV dimensions and improvement of RV strain. Two years after the procedure, the patient was alive and reported sustained clinical improvement (**Table 2**).

CASE 2

A 79-year-old female patient had previously been hospitalized for RV failure. She had severe heart failure symptoms, including dyspnea (NYHA functional class III), peripheral edema, pleural effusions (**Figure 3A**), ascites, chronic renal failure, and elevated N-terminal pro-B-type natriuretic peptide (NT-proBNP) (**Table 2**). TR was massive, as assessed by echocardiography. Stent implantation was uneventful, and at 2-month follow-up, symptomatic improvement had occurred (NYHA functional class II; resolution of peripheral edema, pleural effusion, and ascites; and significant weight loss). CT revealed good position of the prosthesis with thickening of the lumen that was interpreted as excessive endothelialization with possible thrombotic overlay. No relevant change of strain compared with preinterventional CT was observed. CMR 7 months after stent implantation showed a reduction of RV dimensions compared with baseline (**Figures 3B to 3D**), whereas RV ejection fraction remained unchanged. However, CMR cines for assessment of RV function were limited by the presence of fast atrial fibrillation during the examination. After surviving a bout of coronavirus disease-2019, the patient died of terminal RV failure 21 months after the intervention.

CASE 3

An 83-year-old male patient who initially underwent transcatheter aortic valve implantation for treatment of symptomatic severe aortic stenosis had persistent severe TR. Clinically, he presented with extensive anasarca, ascites, and exertional dyspnea (NYHA functional class III). TR was severe (**Figure 4A**) with normal RV function, leading to visible giant bilateral venous systolic reflux into the jugular vein (ie, pulsation formed by fused C and V waves, also called the Lancisi sign [3]) (Video 3A). The patient was undergoing dialysis for chronic renal failure secondary to cardiorenal syndrome. Volume overload of the RV was apparent, and NT-proBNP was elevated. After successful transcatheter implantation of a bicaval

ABBREVIATIONS AND ACRONYMS

4D = 4-dimensional

CMR = cardiac magnetic resonance

CT = computed tomography

NT-proBNP = N-terminal pro-B-type natriuretic peptide

NYHA = New York Heart Association

RA = right atrium

RV = right ventricular

TR = tricuspid regurgitation

TABLE 1 Use of Different Imaging Modalities in the Setting of Transcatheter Bicaval Valved Stent Implantation

Imaging Modality	Preprocedural	Postprocedural
Echocardiography (TTE or alternatively TEE)	TR mechanism and severity Evaluation of eligibility for transcatheter treatment RV function RV and LV function by strain	Positioning of the prosthesis Competence of valve element Paravalvular leakage Patency of liver veins RV and LV function by strain
Computed tomography	Annular and RV dimensions Caval dimensions and height to liver vein junction Eligibility for annuloplasty or caval valve implantation RV and LV function by strain	Positioning of prosthesis Detection of fractures 3D reconstruction and dynamic analyses RV and LV function by strain
Cardiac magnetic resonance	TR severity RV function and dimensions RV and LV function by strain	RV function and dimensions RV and LV function by strain

3D = 3-dimensional; LV = left ventricular; RV = right ventricular; TEE = transesophageal echocardiography; TR = tricuspid regurgitation; TTE = transthoracic echocardiography.

TABLE 2 Clinical and Multimodality Characteristics at Baseline and Follow-up

	Case 1		Case 2		Case 3	
	Baseline 82-Year-Old Woman	Follow-Up 2 Months	Baseline 79-Year-Old Woman	Follow-Up 2 Months	Baseline 83-Year-Old Man	Follow-Up 3 Months
TR severity	Massive	Massive	Massive	Severe	Severe	Massive
Vena contracta (mm)	20	17	14	13	11	18
TAPSE (mm)	14	17	5	11	22	22
sPAP (mm Hg)	27	27	25	25	33	21
NYHA functional class	IV	III	III	II	III	II
Peripheral edema	+++	–	+++	–	+++	–
Ascites	++	–	++	–	+++	–
Weight (kg)	72	57	76	65	93	75
GFR (mL/min)	86	76	25	29	Dialysis	Dialysis
NT-proBNP (pg/mL)	7,372	3,497	4,483	7,978	22,323	11,921
CMR	–	175 d	–	216 d	–	185 d
RVEDV (mL)	331	266	238	218	291	246
RVEF (%)	49	54	55	51	52	51
RV GLS (%)	−17.98	−18.22	−13.59	−10.3	−16.91	−21.98
RV GRS (%)	13.65	15.26	21.85	11.64	15.28	22.78
RV GCS (%)	−9.79	−10.26	−13.59	−8.73	−10.56	−14.46
CT	–	55 d	–	55 d	–	93 d
RV EDA (cm^2)	43.94	36.33	36.47	38.79	54.55	49.65
RV ESA (cm^2)	36.83	29.43	26.3	27.55	43.87	34.09
RV FAC (%)	16.17	18.98	27.88	28.97	19.58	31.34
RV -GLS (%)	−6.07	−8.61	−17.18	−15.23	−7.75	−14.48
RV GRS (%)	16.91	21.18	10.03	23.95	18.53	41.26

Clinical and echocardiographic follow-up reported after 2 and 3 months, respectively. CMR and CT follow-up reported after the given time period (days).

CMR = cardiac magnetic resonance; CT = computed tomography; EDA = end-diastolic area; ESA = end-systolic area; FAC = fractional area change; GCS = global peak systolic circumferential strain; GFR = glomerular filtration rate; GLS = global peak systolic longitudinal strain; GRS = global peak systolic radial strain; LV = left ventricular; NT-proBNP = N-terminal pro-B-type natriuretic peptide; NYHA = New York Heart Association; RV = right ventricular; RVEDV = right ventricular end-diastolic volume; RVEF = right ventricular ejection fraction; sPAP = systolic pulmonary artery pressure; TAPSE = tricuspid annular plane systolic excursion; TR = tricuspid regurgitation.

FIGURE 1 Schematic Measurements and Preprocedural and Postprocedural CT

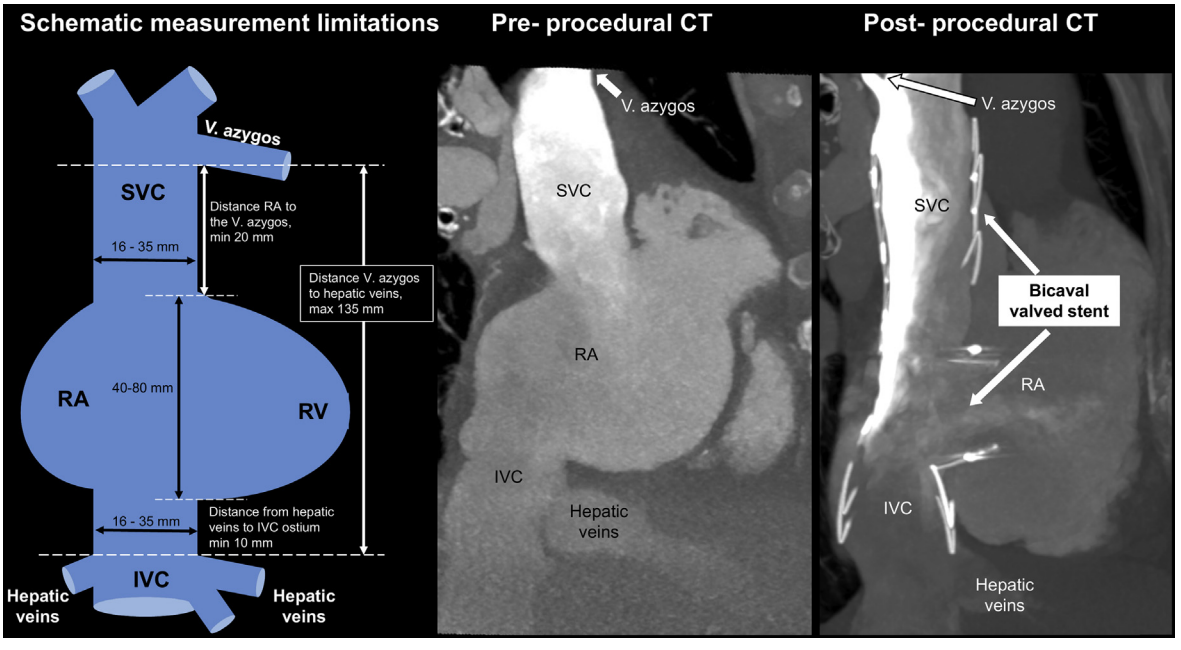

CT = computed tomography; IVC = inferior vena cava; RA = right atrium; RV = right ventricle; SVC = superior vena cava; V. = vena.

FIGURE 2 **Case 1**

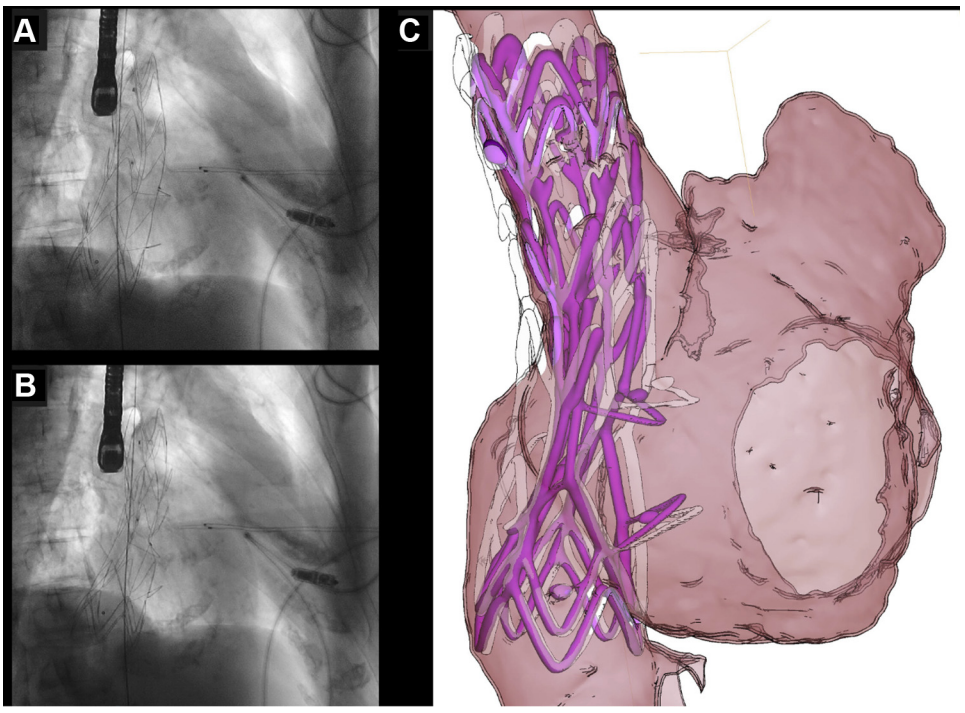

Fluoroscopy after prosthesis deployment in **(A)** diastole and **(B)** systole. **(C)** Computed tomography depicting movement of the prosthesis in systole **(pink)** and diastole **(white)**.

valved stent, the patient experienced relief of heart failure symptoms (NYHA functional class II, resolution of peripheral edema and jugular venous reflux, and weight loss). RV dimensions (RV end-diastolic volume, −18.3% compared with baseline) and NT-pro-BNP decreased (**Figure 4B**), and the Lancisi sign disappeared on both sides after the procedure (Video 3B). A 4D CT scan at 30 days showed correct position of the stent with increased systolic compression resulting from a tangential impact of the regurgitant jet in the RA (Videos 4A and 4B); this led to suspicion of a possible stent fracture. After 21 months, the patient was alive and reported sustained clinical improvement.

CT images and reconstructions were carefully reviewed for all 3 treated patients and in retrospect revealed small fractures of the stent frame in all cases. Fractures were located at the height of the caudal valve element facing the lateral wall of the RA. In all cases, valve function remained intact, and we did not observe any clinical consequences.

DISCUSSION

The implantation of a heterotopic valve in the vena cava may represent a safe and effective therapeutic option aiming to alleviate symptoms in selected patients who are ineligible for surgical repair procedures (4). The reported cases demonstrate the utility of multimodality imaging for preprocedural and postprocedural evaluation, as well as for the detection of device failure. Although echocardiography is used to measure TR severity, CMR is the gold standard for assessing RV dimensions and ejection fraction with high accuracy and reproducibility. Further, CMR strain analysis has the advantage of better characterizing myocardial function (5). To assess anatomical dimensions of the vena cava, vena azygos, and liver veins, as well as their relations with surroundings structures, dedicated 4D CT should be performed because high spatial resolution and 3-dimensional image acquisition overcome the limitations of echocardiography and CMR (6,7). In addition, device po-

FIGURE 3 Case 2

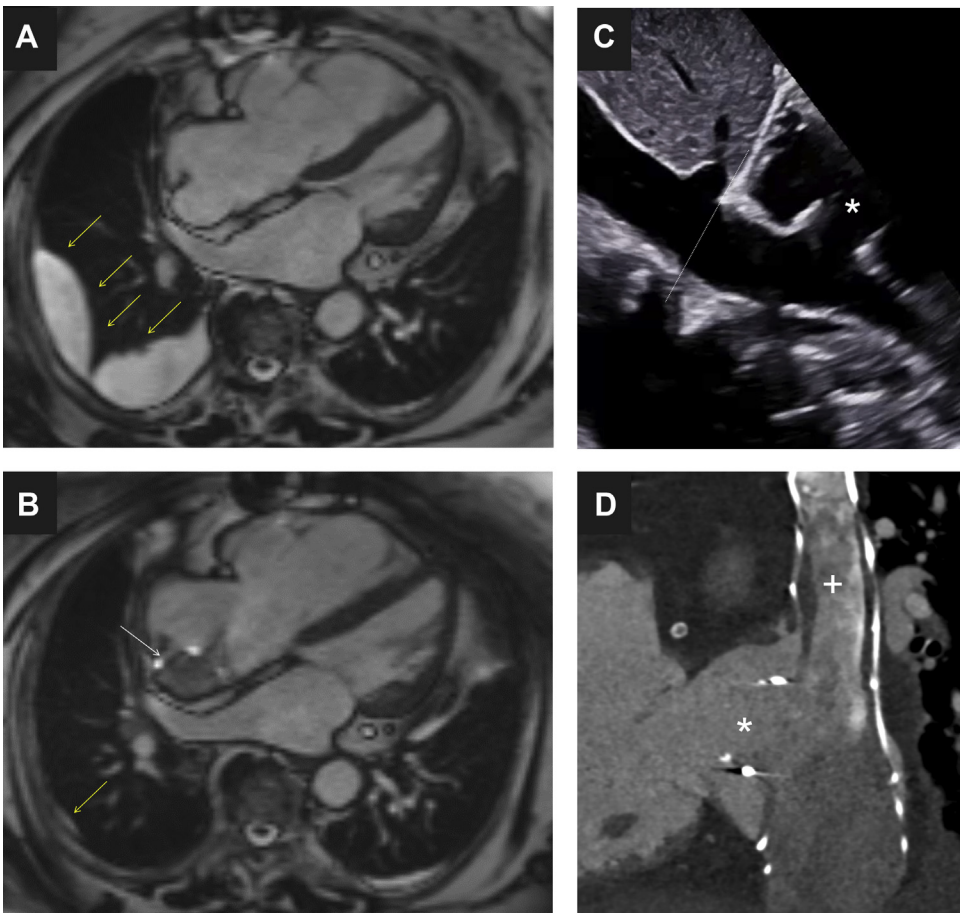

(A) Baseline cardiac magnetic resonance showing pleural effusion **(yellow arrows)** and right ventricular dilation. **(B)** At 6-month follow-up, cardiac magnetic resonance showing resolution of pleural effusion **(yellow arrow)** and reduced right ventricular dimensions (the **white arrow** points to the prosthesis). **(C)** Discharge echocardiography and **(D)** computed tomography follow-up for evaluation of prosthesis positioning ensuring alignment of the caudal prosthesis end with the caval-hepatic vein junction **(C, white dotted line)**; the **asterisk** shows the valve element, and the **plus sign** shows endothelialization of the prosthesis.

sition is better appreciated using CT compared with CMR and echocardiography given the limited echo window of the RA and vena cava. In our serial follow-up, CT allowed us to detect stent fractures that were not evident on echocardiography; however, the fractures did not translate into clinical symptoms or adverse events. In these particular cases, the mechanism of stent fractures may have been explained by the exposure of the prosthesis to the regurgitant jet in the RA. To elucidate this better, we performed 3-dimensional reconstructions and part-comparison analysis with visualization of the shift in systole vs diastole between different parts of the prosthesis depicted on a heat map (Figures 5A and 5B). This postprocessing analysis confirmed that the segments of the stent exposed to the greatest physical stress were those located on the opposite site of the valve. These results were used to optimize the device design by reinforcing the posterior aspect of the stent with the addition of a transverse strut. Further follow-up imaging of patients treated with the first and second generation of the implant will provide information about late consequences, as well as the efficacy of the most recent design modifications.

RV strain values may possibly represent myocardial function more accurately and should be the preferred parameters for monitoring treatment success compared with simple ejection fractions. We were able to show that 4D CT allows not only anatomical evaluation, but also assessment

FIGURE 4 Case 3: Echocardiography

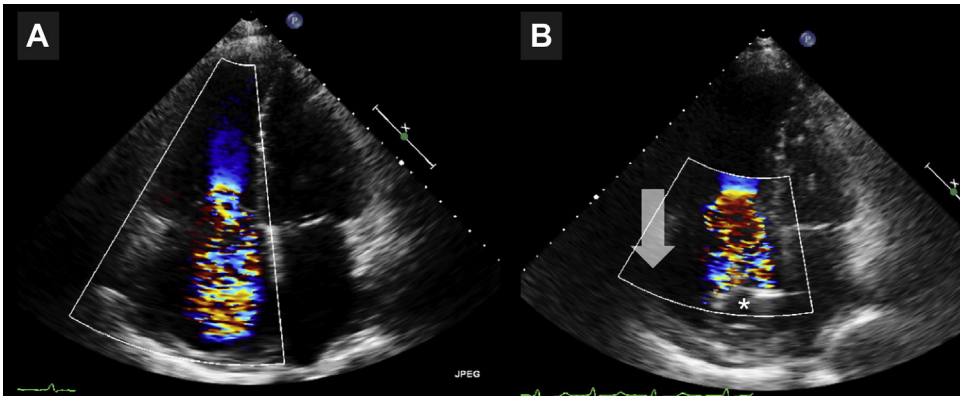

(A) Baseline transthoracic echocardiography with color Doppler showing severe tricuspid regurgitation (4-chamber view). **(B)** Transthoracic echocardiography at 1-month follow-up showing the regurgitant jet tangentially affecting the prosthesis **(asterisk);** the **arrow** shows the direction of the regurgitant jet.

FIGURE 5 Case 3: CT Reconstruction

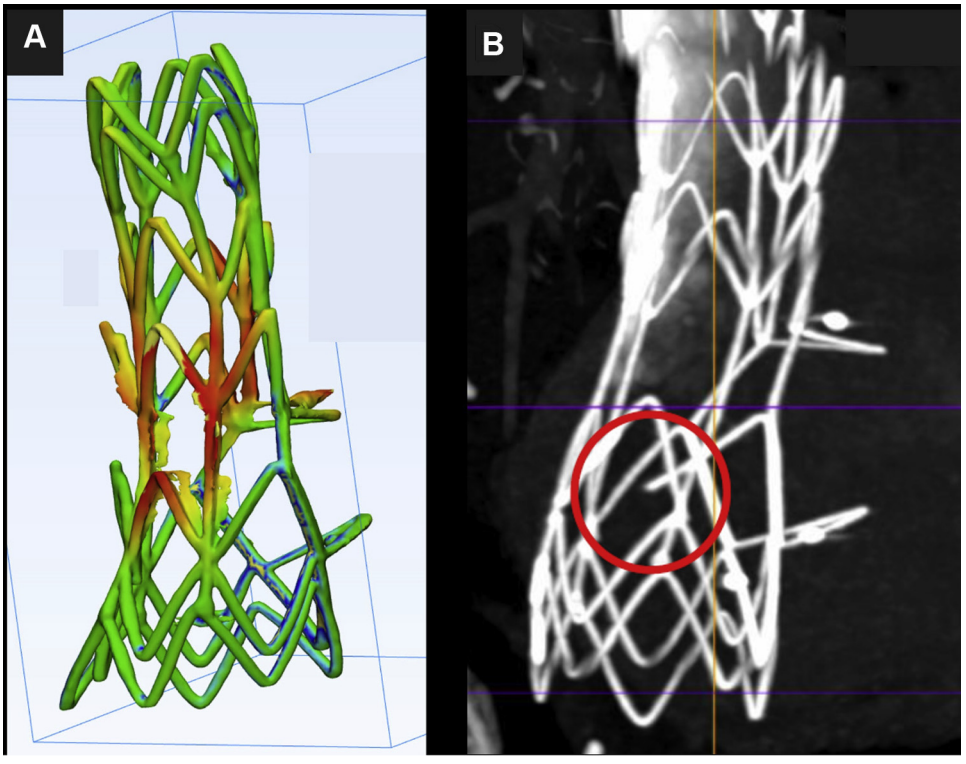

(A) Part comparison and heat map of the prosthesis. **Red** represents maximal deformation of the stent parts (assessed in 30% of the RR interval [ie, systole] vs 80% [ie, diastole]), whereas **green** represents minimal stent part deformation. Maximal deformation is observed on the posterior side of the stent. **(B)** Maximum intensity projection of the computed tomography scan with fracture of the stent frame **(red circle).** Congruent with maximal deformation, the stent fracture is located on the posterior side of the stent.

of RV function using strain imaging, which was concordant with CMR. Accurate postprocedural evaluation of novel devices for detection of subclinical complications is crucial, and 4D CT may offer an "all-in-1" tool for both functional and structural assessments.

CONCLUSIONS

Multimodality imaging is essential for preprocedural planning and result evaluation after transcatheter tricuspid valve interventions. The systematic use of advanced imaging modalities should be encouraged to better assess the procedural result, detect potential subclinical device alterations, and refine device design and patient selection.

FUNDING SUPPORT AND AUTHOR DISCLOSURES

Dr Windecker has received research and educational grants to the institution from Abbott, Amgen, Bristol Myers Squibb, Bayer, Boston Scientific, Biotronik, Cardinal Health, CardioValve, CSL Behring, Daiichi Sankyo, Edwards Lifesciences, Johnson&Johnson, Medtronic, Querbet, Polares, Sanofi, Terumo, Sinomed; has served as an unpaid advisory board member and/or unpaid member of the steering or executive group of trials funded by Abbott, Abiomed, Amgen, AstraZeneca, Bristol Myers Squibb, Boston Scientific, Biotronik, Cardiovalve, Edwards Lifesciences, MedAlliance, Medtronic, Novartis, Polares, Sinomed, V-Wave, and Xeltis; is member of the steering or executive committee group of several investigator-initiated trials that receive funding from industry without an impact on his personal remuneration; and has been an unpaid member of the Pfizer Research Award selection committee in Switzerland. Dr Praz has received payment for travel expenses from Edwards Lifesciences, Abbott Vascular, and Polares Medical. Dr Gräni has received payment for travel expenses from Bayer AG; and has received funding from the Swiss National Science Foundation and InnoSuisse. All other authors have reported that they have no relationships relevant to the contents of this paper to disclose.

ADDRESS FOR CORRESPONDENCE: Dr Christoph Gräni, Department of Cardiology, University Hospital Bern, Freiburgstrasse 10, CH-3010 Bern, Switzerland. E-mail: christoph.graeni@insel.ch. Twitter: @chrisgraeni.

REFERENCES

1. Toggweiler S, De Boeck B, Brinkert M, et al. First-in-man implantation of the Tricento transcatheter heart valve for the treatment of severe tricuspid regurgitation. *EuroIntervention*. 2018;14(7):758–761.

2. Montorfano M, Beneduce A, Ancona MB, et al. Tricento transcatheter heart valve for severe tricuspid regurgitation: procedural planning and technical aspects. *J Am Coll Cardiol Intv*. 2019;12(21):e189–e191.

3. Ali MA, Colquhoun M. Lancisi sign: giant C-V waves in tricuspid regurgitation. *Mayo Clin Proc*. 2020;95(12):2592–2593.

4. Cruz-Gonzalez I, González-Ferreiro R, Amat-Santos IJ, Carrasco-Chinchilla F, Alonso Briales JH, Estévez-Loureiro R. TRICENTO transcatheter heart valve for severe tricuspid regurgitation. Initial experience and mid-term follow-up. *Rev Esp Cardiol (Engl Ed)*. 2021;74(4):351–354.

5. Fischer K, Obrist SJ, Erne SA, et al. Feature tracking myocardial strain incrementally improves prognostication in myocarditis beyond traditional CMR imaging features. *J Am Coll Cardiol Img*. 2020;13(9):1891–1901.

6. Naoum C, Blanke P, Cavalcante JL, Leipsic J. Cardiac computed tomography and magnetic resonance imaging in the evaluation of mitral and tricuspid valve disease: implications for transcatheter interventions. *Circ Cardiovasc Imaging*. 2017;10(3):e005331.

7. Hahn RT, Thomas JD, Khalique OK, Cavalcante JL, Praz F, Zoghbi WA. Imaging assessment of tricuspid regurgitation severity. *J Am Coll Cardiol Img*. 2019;12(3):469–490.

KEY WORDS 3-dimensional reconstruction, caval stent, multimodality imaging, right ventricular strain, Tricento

APPENDIX For supplemental videos, please see the online version of this paper.